The kinetics of mixed Ni-Al hydroxide formation on clay and aluminum oxide minerals: A time-resolved XAFS study

ANDRÉ M. SCHEIDEGGER,[1,2,]* DANIEL G. STRAWN,[1] GERALDINE M. LAMBLE,[3] and DONALD L. SPARKS[1]

[1]Department of Plant and Soil Sciences, University of Delaware, Newark, Delaware 19717-1303, USA
[2]Waste Management Laboratory, Paul Scherrer Institut, CH-5232 Villigen PSI, Switzerland
[3]Earth Sciences Division, Lawrence Berkeley National Laboratory, Berkeley, California 95617, USA

Abstract—In this study kinetic investigations were combined with X-ray Absorption Fine Structure (XAFS) measurements to determine Ni sorption processes on pyrophyllite, gibbsite, and montmorillonite over extended time periods (min-months). The kinetic investigations revealed that Ni sorption reactions (pH = 7.5, $[Ni]_{initial}$ = 3 mM, I = 0.1 M (NaNO$_3$)) were initially fast (8–35% of the initial Ni was removed within the first 40 min). Thereafter, the rate of sorption decreased significantly and depended on the type of mineral surface. For the Ni/pyrophyllite system Ni removal was almost complete after a reaction time of 24h while for the Ni/gibbsite and Ni/montmorillonite systems metal sorption continued up to ≈2 months.

XAFS data revealed the presence of a mixed Ni/Al phase in the Ni/pyrophyllite and Ni/gibbsite systems after a reaction time of minutes. These results suggest that adsorption and nucleation processes (mixed Ni/Al phase formation) can occur simultaneously over time scales of only minutes. However, our finding of a fast growing mixed Ni/Al phase cannot be extrapolated to other sorption systems. A reaction time of 48 h was required for the presence of a mixed Ni/Al phase in the Ni/mormorillonite system. As reaction time progressed, the number of second neighbor Ni atoms (N_{Ni-Ni}) at a distance of ≈3.05 Å increased in all sorption systems, suggesting further growth of a mixed Ni/Al phase with increasing reaction time.

Our study suggests that three phenomena occur at the mineral/liquid interface: (1) nonspecific (i.e, outer-sphere complexation) and/or specific adsorption (i.e., inner-sphere complexation), (2) dissolution of Al, and (3) nucleation of a mixed Ni/Al phase. The rate-limiting step is the dissolution of Al from the surface, which depends on the mineral substrate. Using the Ni linear sorption rates observed in the Ni/gibbsite and Ni/montmorillonite systems and assuming the Ni/Al ratios in our sorption samples are within the range of Ni/Al ratios provided in the literature (1.3–5.6), one can estimate an average Al dissolution rate which seems to be enhanced compared to the Al dissolution rates of the minerals alone. This finding indicates that the dissolution of clay and aluminum oxide minerals can be promoted by metal ions such as Ni(II) through the formation of a mixed Ni/Al phase. *Copyright © 1998 Elsevier Science Ltd*

1. INTRODUCTION

Sorption reactions at the mineral/water interface greatly affect the mobility, speciation, fate, and bioavailability of trace metals in aquatic and soil environments. To definitively understand how these processes are affected and to make sound decisions about environmental remediation, it is imperative that the kinetics and mechanisms of metal sorption reactions be precisely understood.

Over the past several decades surface complexation models have been developed and applied to describe metal sorption reactions at the solid-water interface (Benjamin and Leckie, 1981; Schindler and Stumm, 1987; Hiemstra et al., 1989). One needs to realize, however, that it is not possible to definitively discriminate among the suggested sorption mechanisms without spectroscopic evidence (Sposito, 1986). Recent studies using advanced analytical methods have demonstrated that the sorption of heavy metals on clay and oxide surfaces results in the formation of multinuclear or polynuclear surface phases much more frequently than previously thought. Polynuclear metal hydroxides of Pb, Co, Cu, and Cr(III) on oxides and aluminosilicates have been discerned with XAFS (Charlet and

Manceau, 1992; Fendorf et al., 1994; O'Day et al., 1994a,b, 1996; Papelis and Hayes, 1996). Such polynuclear surface phases have been observed at metal surface loadings far below a theoretical monolayer coverage and in a pH-range well below the pH where the formation of metal hydroxide precipitates would be expected according to the thermodynamic solubility product (Fendorf et al., 1994; O'Day et al., 1994a,b, 1996; Papelis and Hayes, 1996). Possible causes of this such as enhanced surface concentration, reduction of the dielectric constant of water near the surface, and solid solution formation have been discussed (O'Day et al., 1994a; McBride, 1994; Towle et al., 1997).

Recent XAFS studies with Ni(II) and Co(II) have demonstrated that metal sorption on clays and aluminum oxides can result in the formation of mixed-cation hydroxide phases (d'Espinose de la Caillerie et al., 1995; Towle et al., 1997; Scheidegger et al., 1997). Mixed-cation hydroxide phases consist of structures in which divalent and trivalent metal ions are distributed within the same brucite-like octahedral hydroxide layer. The general chemical formula for the compounds is $[Me^{2+}_{1-x}Me^{3+}_x(OH)_2]^{+x} \cdot (x/n)A^{-n} \cdot mH_2O]$, where, for example, Me^{2+} is Mg(II), Ni(II), Co(II), Zn(II), Mn(II), and Fe(II), and Me^{3+} is Al(III), Fe(III), and Cr(III). The compounds exhibit a net positive charge x per formula unit which is

---

*Author to whom correspondence should be addressed (andre. scheidegger@psi.ch).

balanced by an equal negative charge from interlayer anions A^{-n} such as Cl^-, Br^-, I^-, NO_3^-, OH^-, ClO_4^-, and CO_3^{2-}; water molecules occupy the remaining interlayer space (Allmann, 1970; Brindley and Kikkawa, 1979; Hashi et al., 1983; Taylor, 1984). Minerals with the chemical formula given above are classified as the pyroaurite- sjoegrenite group (Hashi et al., 1983). The minerals takovite, $Ni_6Al_2(OH)_{16}CO_3 \cdot H_2O$ and hydrotalcite, $Mg_6Al_2(OH)_{16}CO_3 \cdot H_2O$ are among the most common natural mixed-cation hydroxide compounds containing Al (Taylor, 1984). A detailed review on the synthesis, characterization, natural occurrence, and catalytic properties of mixed-cation hydroxide phases can be found elsewhere (Cavani et al., 1991).

The main focus of previous XAFS studies on Ni and Co sorption on clay and aluminum oxide surfaces has been the characterization of the sorption phase (mixed Ni-Al and Co-Al hydroxide phases; d'Espinose de la Caillerie et al., 1995; Towle et al., 1997; Scheidegger et al., 1997). In the case of Ni, short-term uptake kinetics have been measured (Scheidegger et al., 1997), however, long-term kinetics have not been studied. Furthermore, the previous kinetic investigations were conducted solely on a macroscopic basis and, thus, definitive conclusions about the sorption mechanisms occurring on the clay and aluminum oxide systems with time, could not be assessed. A better approach for determining the sorption mechanisms which result in the formation of mixed metal hydroxide phases is to combine kinetic and spectroscopic investigations. A combination of kinetic and spectroscopic data can provide a better understanding of what chemically happens on an atomic/molecular level over time and thus, can be important in assessing the mobility of metals in the mineral systems over extended time periods (Sparks, 1989, 1995, 1998a,b). To date there are only a few examples in the literature of studies where mechanisms of metalloid sorption reactions on natural components have been hypothesized via kinetic experiments and verified in separate XAFS studies (see e.g., Fuller et al., 1993; Waychunas et al. 1993).

The objective of the present study is to employ XAFS in order to monitor the growth of mixed Ni/Al hydroxide phases on Ni/clay and Ni/aluminum oxide systems as a function of reaction time and to ascertain how the Ni coordination environment changes with time. Thus, short-term and long-term Ni sorption studies were conducted (up to a reaction time of ≈ 2 months). The short-term experiments were conducted directly adjacent to the beamline in order to avoid any possible impact of the storage time on the metal coordination environment prior to the analyses. Furthermore, we will address the question of whether it is possible to spectroscopically distinguish between adsorption (e.g., mononuclear Ni surface complexation) and nucleation processes (mixed Ni/Al hydroxide formation) in our sorption samples treated with Ni for various reaction times. We will also propose a rate-limiting reaction step and discuss the effect of surface loading on the coordination environment and the geochemical impact of our findings.

2. EXPERIMENTAL METHODS

2.1. Materials

The $<2 \, \mu m$ clay fraction of well characterized pyrophyllite and Na-montmorillonite were used. Pyrophyllite shows little deviation from the ideal chemical formula ($Al_2Si_4O_{10}(OH)_2$) of 2:1 clays. A very small substitution of Al for Si can occur which is commonly ≈ 0.001 Al

cations per formula unit (Evans and Guggenheim, 1989). Its dioctahedral structure consists of essentially neutral tetrahedral-octahedral-tetrahedral layers. Hence, the complexity associated with the permanent charge of planar clay surfaces can be avoided and sorption of ions on pyrophyllite can be ascribed to only edge surface sites (Keren and Sparks, 1994). The preparation and characterization of the pyrophyllite is described elsewhere (Scheidegger et al., 1996a). Montmorillonite represents a more complex surface than pyrophyllite and has both external and internal binding sites. Na-montmorillonite was prepared by removing carbonates (4h in Na-acetate buffer at 333K, pH 4.74; Amonette and Zelazny, 1994) and treating the material in dilute (3%) H_2O_2 to remove traces of organic matter (Amonette and Zelazny, 1994). The $<2 \, \mu m$ clay fraction was obtained by centrifuging, washing three times with 0.5 M $NaNO_3$ and removing excess salts by dialysis followed by freeze drying of the clay material. We also used gibbsite ($Al(OH)_3$; Alcoa Co.) which is an important aluminum oxide mineral in soils. Specific adsorption on strongly pH-dependent surface sites is considered to account for the binding of metal ions by the gibbsite surface (Kinniburgh and Jackson, 1981; McBride, 1994). X-ray diffraction (XRD, Philips, PW1729) analysis revealed that the material contains 10% bayerite, a polymorph of gibbsite. Particle size analysis showed that 90% of the material is less than 2 μm.

The specific surface area of the materials was determined by the BET method using N_2 adsorption (pyrophyllite, gibbsite, and montmorillonite) and the ethylene glycol monoethyl ether (EGME) method (Carter et al., 1965). The surface areas were 25 m^2/g (BET) for gibbsite, 95 (EGME) and 96 m^2/g (BET) for pyrophyllite, and 697 m^2/g (EGME) and 15.2 m^2/g (BET) for montmorillonite. The BET method accounts for the external surface area of the minerals, whereas the EGME method accounts for the external and internal surface area. For pyrophyllite the variation between the two methods was small, which demonstrates that no significant amount of swelling clays, such as montmorillonite, was present.

2.2. Batch Studies

Nickel sorption samples were prepared using a batch technique designed to maintain constant pH (pH-stat, Radiometer) and temperature (298 K) and to eliminate CO_2 by purging with N_2. The sorbents were hydrated in a 0.1 M $NaNO_3$ solution (pH = 7.5) for 24 h prior to reaction with Ni. After hydration, the suspension was brought to a solid/liquid ratio of 10 g/L. 18 mL of Ni from a 0.1 M $Ni(NO_3)_2$ stock solution (pH ≈ 6) was dispensed in stepwise additions (within ≈ 5–10 min; aliquots of 0.5 mL) into a large batch reaction vessel (800 mL) in order to avoid the formation of Ni-precipitates due to local oversaturation of the suspension. The suspension was vigorously stirred with a propeller stirrer (Caframo Co.). The pH was automatically held constant (pH = 7.5) and the electrode recalibrated every 24 h. The initial Ni concentration (3 mM) and the reaction pH (pH = 7.5) were selected to achieve considerable sorption densities while ensuring that the bulk solutions were undersaturated with respect to crystalline $Ni(OH_2)$ (s). Nickel speciation revealed that Ni(II) was predominately present as Ni^{2+} (aq.) (Table 1). The concentrations of hydrolysis products such as $Ni(OH)^+$, $Ni(OH)_2^0$, $Ni(OH)_3^-$, $Ni(OH)_4^{2-}$, $Ni_2(OH)^{3+}$, and $Ni_4(OH)_4^{4+}$ are low. Solution speciation suggests the solubility of $Ni(OH)_2(s)$ at the conditions employed is reached at a [Ni] of 7.727 $\times$ 10^{-3} M. One can argue that there is a significant variation of reported log K_{sp} values for $Ni(OH)_2(s)$ in the literature (-10.99 to -18.06; Mattigod et al., 1997). A recent study investigated the solubility of $Ni(OH)_2(s)$ as a function of pH and reaction time in great detail. The study revealed that the [Ni] in a supersaturated system at pH = 7.5 (0.01 M $NaClO_4$) was $>3 \times 10^{-3}$ M even after a reaction time of 90 days (Mattigod et al., 1997). The maximum [Ni] in our sorption systems remaining in solution after a reaction of ≈ 2–3 months is $<6 \times 10^{-4}$ M (Ni montmorillonite system, see Fig. 1c). Thus, one can assume that Ni removal from solution is not due to $Ni(OH)_2(s)$ formation in solution at any time during the experiments. This assumption will later on be confirmed by the XAFS measurements (section 3.4).

In an effort to follow changes in the local atomic structure of sorbed Ni ions as a function of short- term reaction time (15 min-24 h), the Ni sorption experiment with pyrophyllite was conducted at the NSLS (Brookhaven National Laboratory, Upton, NY). By conducting kinetic

Table 1. Solution speciation for 3×10^{-3} M Ni in aqueous solution (0.1 M $NaClO_4$) at pH = 7.5 as predicted by MINEQL (Westall et al., 1976).

Species (aq)	[c] M	log Ksp[a]	Reference
Ni^{2+}	2.99×10^{-3}		
$Ni(OH)^+$	8.81×10^{-6}	-9.71	Wagman et al., 1982
$Ni(OH)_2^0$	1.12×10^{-8}	-20.0	Smith and Martell, 1976
$Ni(OH)_3^-$	4.52×10^{-11}	-30.0	Baes and Mesmer, 1976
$Ni(OH)_4^{2-}$	2.99×10^{-17}	-44.0	Baes and Mesmer, 1976
$Ni_2(OH)^{3+}$	7.22×10^{-9}	-10.7	Baes and Mesmer, 1976
$Ni_4(OH)_4^{4+}$	1.46×10^{-8}	-27.74	Baes and Mesmer, 1976
		log Ksp[b]	
$Ni(OH)_2(s)$		-12.73	Wagman et al., 1982

[a] For hydrolysis, equilibrium constants are for the reaction
$xNi^{2+} + yH_2O = Ni_x(OH)^{(2-y)} + yH^+$

[b] Solubility constant for the reaction $Ni(OH)_2(s) = Ni^{2+} + 2OH^-$

studies at the NSLS, XAFS samples could be immediately measured and any possible influence of storage time on the metal coordination environment prior to XAFS measurements could be circumvented. The Ni sorption experiment on pyrophyllite was conducted at approximately 303 K. Collected samples were passed through a 0.22 μm membrane filter, and the supernatant was analyzed by inductively coupled plasma emission (ICP) spectrometry for Ni. The remaining wet pastes (0.8 g solid in approx. 2–3 mL trapped solution) were immediately washed with 20mL high-purity water to adequately remove electrolyte and Ni in the entrained solution (see below) and then filtered again. The washing process was repeated twice. The wet pastes were then mounted on a sample holder for XAFS analysis.

Because Ni sorption on montmorillonite and gibbsite exhibit much slower sorption kinetics, the experiments were conducted in our laboratory rather than directly at the NSLS. After a reaction time of 1 week, the suspensions were poured into a vial. The vial was sealed and kept at 298 K in a dessicator containing granulated sodium hydroxide to adsorb CO_2. The suspensions were shaken from time to time and the pH was readjusted. Samples were collected, centrifuged, and the supernatant was passed through a 0.22 μm membrane filter and analyzed for Ni by ICP spectrometry. For the Ni/gibbsite system the remaining wet pastes were washed with excess high-purity water to adequately remove Ni and electrolyte in the entrained solution (see below) and then centrifuged again. Again, the washing process was repeated twice. For the Ni/montmorillonite system the remaining wet pastes were washed once with 0.1M $NaNO_3$ (pH = 7.5). The samples were then sealed and stored for 1–5 weeks in a refrigerator to keep them moist prior to XAFS analysis.

It must be realized that the washing procedures employed (Ni/pyrophyllite and Ni/gibbsite systems: washing with high-purity water; Ni/montmorillonite system: washing with 0.1 M $NaNO_3$) were not ideal and did possibly remove not only nonsorbed Ni in the entrained solution but also some loosely-bound or easily-exchangeable Ni-complexes (e.g., outer-sphere complexes which are easily exchanged by Na^+ on the cation exchangeable sites of montmorillonite). ICP measurements of the washing solutions revealed that the amount of desorbed loosely-bound or easily-exchangeable Ni-complexes in the Ni/pyrophyllite and Ni/gibbsite systems was small (<5% of the total sorbed amount desorbed). In the Ni/montmorillonite system, however, the washing procedure resulted in up to 20% of the sorbed amount of Ni being desorbed during washing. A significant part of the desorbed Ni might have been loosely-bound. Thus, the washing procedure possibly shifted the fraction of Ni observed with XAFS to strongly-bound complexes, either on the surface or in a new solid phase. Nevertheless, the washing procedure with 0.1 M $NaNO_3$ was chosen in order to remove Ni in the entrained solution while avoiding a decrease in the ionic strength. Washing with high-purity water would decrease the ionic strength and a decrease in the ionic strength in the Ni/montmorillonite system would result in further metal uptake (Papelis and Hayes, 1996). Furthermore, it results (through an expansion of the interlayers) in dilute slurry-like wet pastes which are not suitable for packing into XAFS sample holders.

2.3. XAFS Studies

XAFS spectra were recorded at beamline X-11A at the NSLS. A Si (111) crystal was employed in the monochromator. Nickel-edge data were collected using a Co-3μm filter. Harmonics were suppressed by detuning 25% from the maximum intensity. Beam energy was calibrated by assigning the first inflection on the K absorption edge of a nickel metal foil to an energy of 8333 eV. The spectra were collected in fluorescence mode using a Stern-Heald-type detector which is available commercially (The EXAFS Co.) and known as a Lytle detector. Fill-gases used were Ar for the Lytle detector and N_2 for the I_o detector. The spectra were collected at 77 K to reduce dampening of the XAFS oscillation by thermal disorder. Comparisons of spectra recorded at 77 K and room temperature revealed no change in structural information while the signal-to-noise ratio was maximized by lowering the temperature (Charlet and Manceau, 1992; Fendorf et al., 1994; Papelis and Hayes, 1996). It should be realized, however, that such findings can not be generalized and extrapolated to other sorption systems. Bargar et al. (1997) have demonstrated that sample freezing can lead to perturbations of sorbed species in samples containing mixtures of adsorbed species and precipitates. Similar observations were made by Lewis and Ratner (1993) who studied the effects of sample freezing on surface rearrangement of polymers using electron spectroscopy for chemical analysis (ESCA). Reference compounds (β-Ni(OH)$_2$ (Johnson Mattey Co) and takovite (Ni$_6$Al$_2$(OH)$_{16}$CO$_3 \cdot$ H$_2$O, Kambalda W. A., Australia)) were lightly crushed to powders with an agate mortar and pestle and diluted with boron nitride to obtain a 1wt% mixture. Details on the experimental setup can be found elsewhere (Scheidegger et al., 1996a).

Background subtraction and Fourier filtering were performed with the Macintosh version of the University of Washington/Naval Research Laboratory data analysis package (MacXAFS, Version 4.0; Bouldin et al., 1995). The χ function was extracted from the raw data using a linear preedge background and spline postedge background and normalizing the spectra near the edge to unity (McMaster et al., 1968). The data were then converted from energy to k space by assigning E_o, the energy at which k = 0, to the inflection point of the K absorption edge. The data were then weighted by k^3 in order to compensate for the damping of the XAFS amplitude with increasing k. McMaster corrections (McMaster et al., 1968) and fill-gas correction (Bunker, 1988) were applied to the experimental data.

Structural parameters were extracted with fits to the standard EXAFS equation. Data analysis was accomplished using the XFTools supplement to MacXAFS (Boyanov, 1997). Ab initio amplitude and phase functions were calculated using the FEFF6 code (Zabinsky et al., 1995) in combination with ATOMS, a program which is part of the University of Washington XAFS analysis package. Single-shell data for the atomic pairs of interest were generated from FEFF6 and were Fourier filtered over ranges identical to those used in the fits. The amplitude of the theoretical data was additionally adjusted by a constant factor determined from fits to the experimental data from reference compounds. Multishell k-space fits were performed over $\Delta R = 1.07$–3.12 Å and $\Delta k = 3.2$–14 Å^{-1} where Δk is the range of k-space being fit, and ΔR
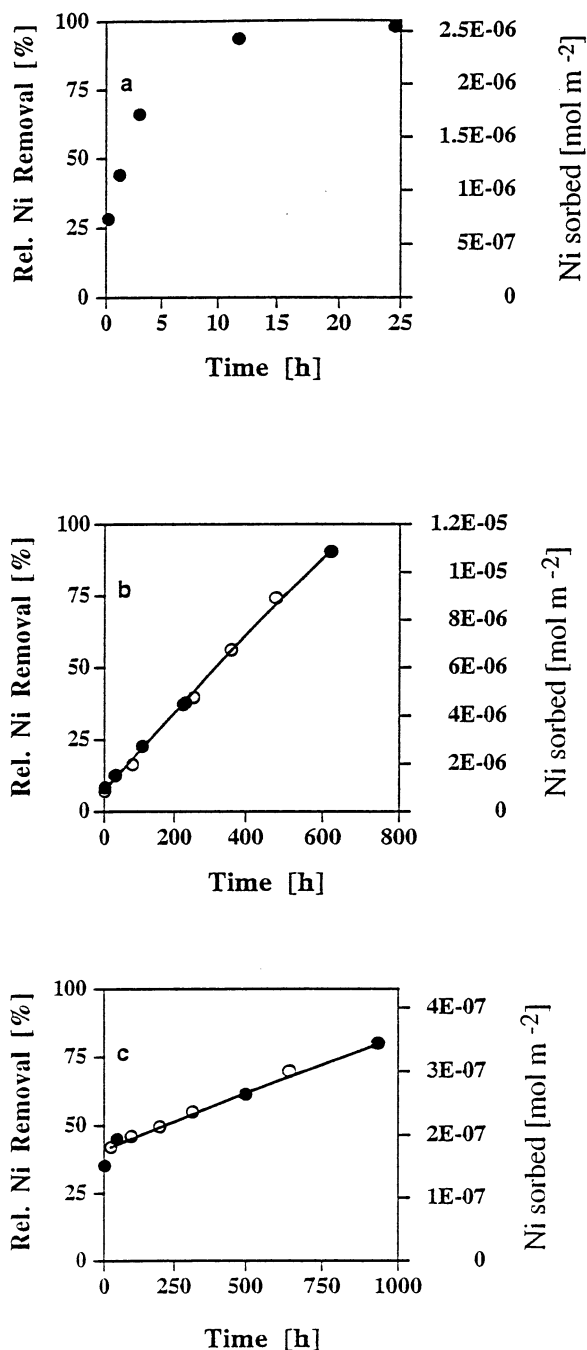
Fig. 1. Kinetics of Ni sorption on pyrophyllite (a), gibbsite (b), and montmorillonite (c) from a 3 mM Ni solution at pH = 7.5 and an ionic strength I = 0.1 M (NaNO₃). Relative Ni removal (%) and the amount of sorbed Ni (mol m⁻²) are shown as function of reaction time (h). The filled circles (●) denote samples which were used for XAFS measurements. The solid lines in (b) and (c) represent a linear fit over the time range of 40 min to 620 h (gibbsite), and 26–930 h (montmorillonite).

is the R-range in the Fourier transform. For the Ni-sorption samples, the Debye-Waller factors for the Ni-Ni and Ni-Al shells were fixed at 0.005 Å², a value which has previously been used to fit a precipitated phase consisting of Co and Al (Towle et al., 1997). The threshold energy was shifted by a small value of ΔE_o, which was minimized during the curve-fitting procedure. The number of parameters used to fit

the data was 8 and never exceeded the total number allowed to vary, according to $N_{free} = 2\Delta k \Delta R/\Pi$, where N_{free} is the number of degrees of freedom (Teo, 1986). Confidence limits for the fitting parameters were calculated as $\epsilon_I = (0.1 * C_{ij})^{1/2}$ where C_{ij} are the diagonal elements of the covariance matrix of the fit. These confidence limits correspond to deviations of parameters from the optimal values which increase the fit residuals by 10% when all other parameters are floated. They illustrate the precision or a statistical analysis of the least-square fits (Boyanov, 1997).

Derived XAFS parameters were tested by fitting β-NiOH₂ and takovite (Table 2). Table 2 reveals that the structural parameters of β-Ni(OH)₂ agree well with XAFS, XRD, and neutron diffraction (ND) derived values reported in the literature. Takovite (Ni₆Al₂(OH)₁₆CO₃·H₂O), is a natural occuring mixed Ni/Al phase whose structure is not as well-defined as those of well-characterized crystalline model compounds. Nevertheless, the XAFS derived Ni-Ni bond distances are close to those observed from XRD. We fitted the spectrum of takovite by (1) fixing the Debye-Waller factors at 0.005 Å², and (2) by constraining Ni-Ni and Ni-Al distances and Debye-Waller factors to be equal. d'Espinose de la Caillerie et al. (1995) suggested that this constraint was dictated by the hydrotalcite structure of mixed Ni/Al hydroxide phases and the assumption that Ni and Al backscatterers play similar roles in the octahedral layers. Table 2 reveals no significant difference in bond distances and coordination numbers for takovite between the two fitting procedures except that the precision is large (±0.06 Å) in the case where no distance constraint was employed.

Table 2 also compares XAFS-derived structural parameters of a Ni/Al coprecipiate (Ni/Al ratios of 3) with those determined independently by XRD. Again, a good agreement between the two methods is observed. One should also notice that Ni-Ni and Ni-Al distances and Debye-Waller factors have been constrained to be equal during XAFS fitting.

Based on data shown in Table 2 we estimate the $R_{(Ni-O)}$ and $R_{(Ni-Ni)}$ to be accurate to ±0.020 Å, the $N_{(Ni-O)}$ and $N_{(Ni-Ni)}$ values to be accurate to ±20%, and the ΔE_o values to ±20%. Due to amplitude cancellation between the Ni and Al shells, the estimated accuracies for $N_{(Ni-Al)}$ and $R_{(Ni-Al)}$ are poorly constrained. We estimate accuracies for $N_{(Ni-Al)}$ and $R_{(Ni-Al)}$ to be at least in the range of the calculated precision ($N_{(Ni-Al)}$ ± 60%; $R_{(Ni-Al)}$ ± 0.06 Å). The sensitivity of XAFS towards the Al contribution in mixed Ni/Al phases has been addressed in detail elsewhere (d'Espinose de la Caillerie et al., 1995; Scheidegger et al., 1997).

Our XAFS data suggest that the Ni coordination environment was preserved after the sorption reaction was quenched (i.e., Ni left in solution was removed) and that conducting the Ni sorption experiment on pyrophyllite directly adjacent to the beamline was not necessary in our study. A few Ni treated pyrophyllite samples were rerun after storing them as wet pastes in a sealed container for 2–3 months at 277 K. No change in the structural Ni parameters could be detected. Furthermore, the data for the Ni/gibbsite and Ni/montmorillonite systems did not reveal any dependence on the storage time (1–5 weeks) once Ni left in solution was removed. Changes in structural parameters were strictly related to the reaction time. To summarize, the data suggest that once the sorbate left in solution is removed by the employed washing process sample storage of the wet pastes prior to data analysis did not change the metal coordination environment in our study.

3. RESULTS

3.1. Nickel Sorption Kinetics

Figure 1 illustrates the kinetics of Ni sorption on pyrophyllite, gibbsite, and montmorillonite from a 3mM Ni solution at pH = 7.5. Relative Ni removal (%) and the amount of sorbed Ni (mol m⁻²) are shown as function of reaction time (h). Figure 1a shows that Ni sorption on pyrophyllite was initially rapid and then decreased gradually. Within the first 15 min 28% (0.7 µmol m⁻²) of the Ni was sorbed. Thereafter the reaction slowed down considerably, with 67% sorbed after a reaction time of 3 h, and nearly complete Ni removal after 24 h (97% sorbed). All collected samples in the Ni/pyrophyllite system were analyzed by XAFS. In addition, we also measured Ni

Table 2: Structural parameters of β-Ni(OH)$_2$, takovite, and a coprecipitated phase containing Ni and Al (Ni/Al ratio = 3) as derived from XAFS analysis in comparison with corresponding values determined by X-ray diffraction (XRD) and neutron diffraction (ND).

	Methods of Analysis	Ni-O (a)			Ni-Ni (a)			Ni-Al (a)			ΔE_0 (a) (eV)	Reference
		R (Å)	N	$\Delta\sigma^2$ (Å2) 10^{-3}	R (Å)	N	$\Delta\sigma^2$ (Å2) 10^{-3} (c)	R (Å)	N	$\Delta\sigma^2$ (Å2) 10^{-3}		
β-Ni(OH)$_2$	XAFS	2.064±0.002	5.6±0.2	3.0±0.3	3.129±0.001	6.0±0.2	3.6±0.2				3.0±0.4	this study
β-Ni(OH)$_2$	XAFS	2.05	5.1	4.0	3.12	5.2	3.2				4.0	d'Espinose de la Caillerie et al., 1995
Ni(OH)$_2$	XAFS	2.06	5.6	6.1	3.125	6.2	6.8					O'Day et al., 1994c
Ni(OH)$_2$	XAFS	2.05	6.0(e)		3.09	6.0(e)						Manceau and Calas, 1986
β-Ni(OH)$_2$	XRD	(d)			3.126							d'Espinose de la Caillerie et al., 1995
Ni(OH)$_2$	XRD	2.07			3.12							Oswald and Asper, 1977
Ni(OH)$_2$	ND	2.121			3.13							Szytula et al., 1971
Takovite (b)	XAFS	2.046±0.004	5.1±0.4	2.6±0.4	3.039±0.007	3.8±0.8	5	3.043±0.06	1.8±1.2	5	4.4±0.4	this study
Takovite (c)	XAFS	2.047±0.004	5.2±0.4	2.7±0.4	3.040±0.006	4.0±0.8	5.4±0.9	3.040±0.006	1.9±1.1	5.4±0.9	4.2±0.9	this study
Takovite	XRD	(d)			3.025							Bish and Brindley, 1977
Ni/Al =3 (c)	XAFS	2.05	6.5	7.3	3.06	4.8	7.8	3.06	1.4	7.8	-3.1	d'Espinose de la Caillerie et al., 1995
Ni/Al =3	XRD	(d)			3.041							d'Espinose de la Caillerie et al., 1995

(a) N, R, $\Delta\sigma^2$ and ΔE_0 stand for the coordination numbers, interatomic distances, Debye-Waller factors and inner potential corrections.
(b) The Debye-Waller factors for the Ni-Ni and the Ni-Al shells were fixed at 0.005 Å^2
(c) Ni-Ni and Ni-Al distances and Debye-Waller factors were constrained to remain equal during fitting (see section 'Experimental Methods').
(d) Not reported
(e) Fixed parameters
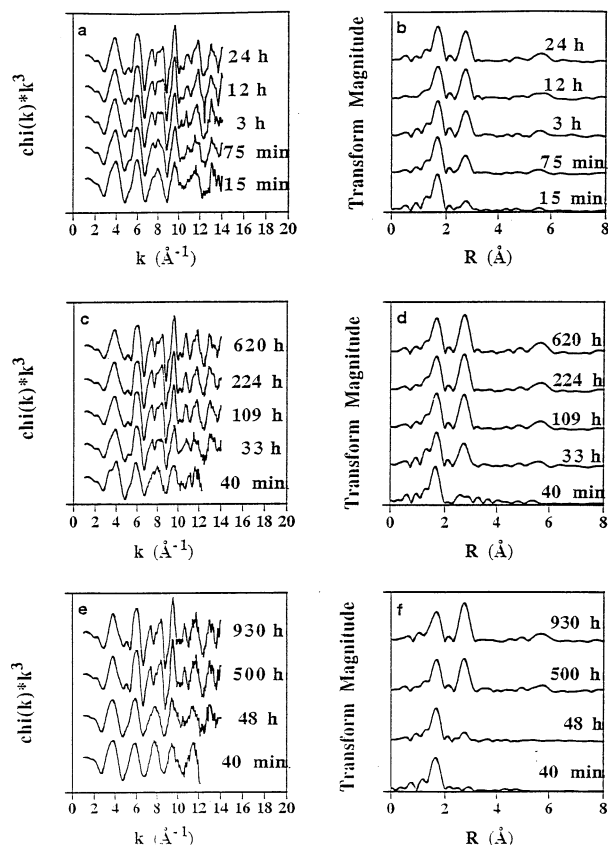
Fig. 2. k^3-weighted, normalized, background-subtracted XAFS spectra of (a) Ni/pyrophyllite, (c) Ni/gibbsite, and (e) Ni/montmorillonite after treatment with Ni for different reaction times. Fourier transforms (uncorrected for phase shift) of (b) Ni/pyrophyllite, (d) Ni/gibbsite, and (f) Ni/montmorillonite corresponding to the XAFS spectra. Note the growth of a peak at a R of about 2.7 Å with increasing reaction time.

that the Ni/gibbsite sorption kinetics differs distinctively from that of Ni/pyrophyllite (Fig. 1a). A constant Ni sorption rate was observed following a first fast sorption step ($\approx$8 % or 1.01 μmol m^{-2} sorbed after 40 min). After approximately 4 weeks 91% of the initial Ni was sorbed. The Ni/montmorillonite sorption kinetics exhibited similar behavior (Fig. 1c) with 35% or 0.152 μmol m^{-2} sorbed within the first 40 min and 80% or 3.45 μmol m^{-2} sorbed after a reaction time of $\approx$6 weeks.

3.2. Changes of the Nickel Coordination Environment with Time as Monitored by XAFS

Normalized, background-subtracted and k^3-weighted XAFS spectra of Ni sorbed on pyrophyllite, gibbsite, and montmorillonite are shown in Fig. 2a,c,e. The XAFS samples for the Ni/pyrophyllite system (Fig. 2a; reaction time: 15 min, 75 min, 3h, 12h, and 24h) were measured immediately after collection (see Experimental Methods). With increasing reaction time one can observe an increasing XAFS out to higher energies which indicates the presence of heavy backscatterer elements such as Ni (Fig. 2a). An increasing XAFS out to higher energies with increasing reaction time is also observed for the Ni/gibbsite system (Fig.2c; reaction time: 40 min, 33 h, 109 h, 224 h, and 620 h) and the Ni/montmorillonite system (Fig. 2e; reaction time: 40 min, 48 h, 500 h, and 930 h).

Figure 2b,d,f illustrates radial structure functions (RSFs) produced by forward Fourier transforms of the XAFS spectra represented in Fig. 2a,c,e. The spectra are uncorrected for phase shift. All spectra show a peak at R $\approx$ 1.8 Å which represents the first coordination shell of Ni. A second peak representing the second Ni coordination shell can be observed at R $\approx$ 2.8 Å in the spectra of all Ni sorption samples (Fig. 2b,d,f) except for the Ni/montmorillonite sample treated with Ni for 40 min (Fig. 2f).

Figure 2b,d,f reveals that as reaction time progressed, and relative Ni removal from solution increased, the peak at R $\approx$ 2.8 Å in the RSFs increased in intensity. This finding reflects an increasing Ni-Ni backscattering contribution with increasing reaction time. The figures also show peaks beyond the second shell at R $\approx$ 5–6 Å. These peaks resulted from multiple scattering among Ni atoms (O'Day et al., 1994b, Papelis and Hayes, 1996) and will not be discussed further.

The structural parameters derived from XAFS analysis are

sorption for 3 months at similar reaction conditions (pH = 7.5 and I = 0.1 M NaNO$_3$; resulting sorption density: 3.1 μmol m^{-2}) in our laboratories.

The kinetics of Ni sorption on gibbsite and montmorillonite are shown in Fig. 1b-c. The closed symbols in the figures denote samples collected for XAFS analysis. Figure 1b reveals

Table 3: Structural parameters of Ni/pyrophyllite samples as derived from XAFS analysis using *XFTools*[a,b].

	relative Ni removal [%]	sorption density, Γ μmol/m^2	Ni-O R (Å)	Ni-O N	Ni-O $\Delta\sigma^2$ (Å^2)	Ni-Ni R (Å)	Ni-Ni N	Ni-Ni $\Delta\sigma^2$ (Å^2) (c)	Ni-Al R (Å)	Ni-Al N	Ni-Al $\Delta\sigma^2$ (Å^2) (c)	ΔE_0 (eV)
15 minutes	28	0.7	2.05	6.0	0.0034	3.06	2.0	0.005	3.08	1.7	0.005	3.3
75 minutes	44	1.1	2.05	6.1	0.0036	3.05	3.2	0.005	3.07	2.0	0.005	4.3
3 hours	67	1.7	2.05	5.3	0.0027	3.06	4.3	0.005	3.11	2.0	0.005	3.8
12 hours	93	2.4	2.05	4.8	0.0025	3.05	5.3	0.005	3.08	3.1	0.005	3.9
24 hours	97	2.6	2.05	5.5	0.0029	3.05	4.9	0.005	3.08	1.7	0.005	4.0
3 months	--	3.1	2.04	5.5	0.003	3.05	6.3	0.005	2.10	4.0	0.005	5.4

(a) N, R, $\Delta\sigma^2$ and ΔE_0 stand for the coordination numbers, interatomic distances, Debye-Waller factors and inner potential corrections.
(b) Estimated accuracies: $R_{(Ni-O)}$ ±0.02 Å, $N_{(Ni-O)}$ ±20%, $R_{(Ni-Ni)}$ ±0.02 Å, $N_{(Ni-Ni)}$ ±20%, $R_{(Ni-Al)}$ ±0.06 Å, $N_{(Ni-Al)}$ ±60%, ΔE_o ±20% (See Section 2).
(c) The Debye-Waller factor was fixed at 0.005 Å^2 for these shells.

Table 4: Structural parameters of Ni/gibbsite samples as derived from XAFS analysis using XF*Tools*[a,b].

	relative Ni removal [%]	sorption density, Γ $\mu mol/m^2$	Ni-O R (Å)	N	$\Delta\sigma^2$ ($\mathring{A}^2$)	Ni-Ni R (Å)	N	$\Delta\sigma^2$ ($\mathring{A}^2$) (c)	Ni-Al R (Å)	N	$\Delta\sigma^2$ ($\mathring{A}^2$) (c)	ΔE_O (eV)
40 minutes	8	1.01	2.06	6.4	0.0041	3.05	2.7	0.005	3.07	4.0	0.005	3.4
33 hours	13	1.53	2.05	6.3	0.0046	3.05	3.9	0.005	3.07	1.2	0.005	4.2
109 hours	23	2.74	2.05	6.0	0.0036	3.06	5.7	0.005	3.09	2.4	0.005	4.8
224 hours	37	4.56	2.05	6.0	0.0038	3.06	6.0	0.005	3.10	2.2	0.005	4.9
620 hours	91	10.89	2.04	5.8	0.0036	3.06	6.6	0.005	3.10	3.1	0.005	4.5

(a) N, R, $\Delta\sigma^2$ and ΔE_O stand for the coordination numbers, interatomic distances, Debye-Waller factors and inner potential corrections.

(b) Estimated accuracies: $R_{(Ni-O)}$ ±0.02 Å, $N_{(Ni-O)}$ ±20%, $R_{(Ni-Ni)}$ ±0.02 Å, $N_{(Ni-Ni)}$ ±20%, $R_{(Ni-Al)}$ ± 0.06 Å, $N_{(Ni-Al)}$ ±60%, ΔE_O ±20% (see Section 2).

(c) The Debye-Waller factor was fixed at 0.005 $\mathring{A}^2$ for these shells.

summarized in Table 3–5. XAFS analysis suggested that in the first coordination shell Ni is surrounded by 6 O atoms. This behavior indicated that Ni(II) is in an octahedral environment. The Ni-O bond distance ($\approx$2.05 Å) and coordination numbers were not affected by the reaction time.

Data analysis of the second coordination shell revealed that the number of second-neighbor Ni atoms (N_{Ni-Ni}) increased with increasing reaction time (Table 3–5). For the Ni/pyrophyllite system N_{Ni-Ni} increased from N = 2.0–6.3 as the reaction time increased from 15 min to 3 months (Table 3) and for the Ni/gibbsite system N_{Ni-Ni} increased from N = 2.7–6.6 as the reaction time increased from 40 min to 620 h (Table 4). For both Ni sorption systems the Ni-Ni bond distances (3.05–3.06 Å) were unaffected by the reaction time.

The Ni/montmorillonite system behaved differently then the Ni/pyrophyllite and Ni/gibbsite systems. The Ni/montmorillonite system lacks a second Ni shell after a reaction time of 40 min (Table 5). This finding indicates the absence of a mixed Ni/Al phase in the XAFS sample. A reaction time of 48 h was required for the appearance of a Ni-Ni backscattering contribution in the Ni/montmorillonite system. As the reaction time increased further (48–930 h) the number of Ni second-neighbor (N) atoms at a distance of 3.06–3.07 Å increased from N = 1.9–6.5.

XAFS analysis suggested the presence of 1.7–4.0 second-neighbor Al atoms for the Ni/pyrophyllite system (Table 3), 1.2–4.0 second-neighbor Al atoms for the Ni/gibbsite system (Table 4), and 0.8–1.5 second-neighbor Al atoms for the Ni/

montmorillonite system (Table 5). For all sorption systems the Ni-Al bond distances (3.07–3.11 Å) were 0.02–0.05 Å longer then the derived Ni-Ni bond distances. However, as elaborated in section 2 (Experimental Methods), the estimated accurrancies for $N_{(Ni-Al)}$ and $R_{(Ni-Al)}$ are poorly constrained due to amplitude cancellation between the Ni and Al shells.

Figure 3a-c shows a comparison of k^3-weighted XAFS functions for the Fourier back-transformed spectra to the theoretical spectra derived with parameters from analysis of the isolated shells (Table 3–5). A good agreement between the Fourier back-transformed XAFS function and the theoretical fit is observed. An unusual asymmetry is visible in the first major oscillation (at $\approx$3.6 $\mathring{A}^{-1}$) in the normalized XAFS spectrum of gibbsite treated with Ni for 40 min and less pronounced in the spectrum of gibbsite treated with Ni for 33 h (Fig. 2c). Although not addressed by the authors, an almost identical asymmetry in the first major oscillation is recognizable in some XAFS spectra of mixed Ni/Al and Co/Al hydroxide phases formed upon Ni or Co sorption onto aluminum oxides (d'Espinose de la Caillerie et al., 1995; Towle et al., 1997). Such an asymmetry in the first major oscillation can indicate some disorder or difference in interatomic distances in the Ni-O and Co-O shell. Although there is possibly some indication of a slightly higher disorder in the XAFS-derived data (Table 4, this study; Towle et al., 1997), the available data do not allow one to draw any conclusions about the significance and cause of this apparently real asymmetric feature in the first major oscillation. However, Fig. 3b reveals that filtering the data over the

Table 5: Structural parameters of Ni/montmorillonite samples as derived from XAFS analysis using *XFTools*[a,b].

	relative Ni removal [%]	sorption density, Γ $\mu mol/m^2$	Ni-O R (Å)	N	$\Delta\sigma^2$ ($\mathring{A}^2$)	Ni-Ni R (Å)	N	$\Delta\sigma^2$ ($\mathring{A}^2$) (c)	Ni-Al R (Å)	N	$\Delta\sigma^2$ ($\mathring{A}^2$) (c)	ΔE_O (eV)
40 minutes	35	0.152	2.05	6.4	0.0041							4.3
48 hours	45	0.194	2.04	5.9	0.0029	3.06	1.9	0.005	3.10	1.5	0.005	4.9
500 hours	61	0.262	2.05	5.2	0.0022	3.07	5.5	0.005	3.11	0.8	0.005	4.8
930 hours	80	0.345	2.04	6.1	0.0041	3.07	6.5	0.005	3.11	1.0	0.005	3.9

(a) N, R, $\Delta\sigma^2$ and ΔE_O stand for the coordination numbers, interatomic distances, Debye-Waller factors and inner potential corrections.

(b) Estimated accuracies: $R_{(Ni-O)}$ ±0.02 Å, $N_{(Ni-O)}$ ±20%, $R_{(Ni-Ni)}$ ±0.02 Å, $N_{(Ni-Ni)}$ ±20%, $R_{(Ni-Al)}$ ±0.06Å, $N_{(Ni-Al)}$ ±60%, ΔE_O ±20% (see 'Results' Section).

(c) The Debye-Waller factor was fixed at 0.005 $\mathring{A}^2$ for these shells.
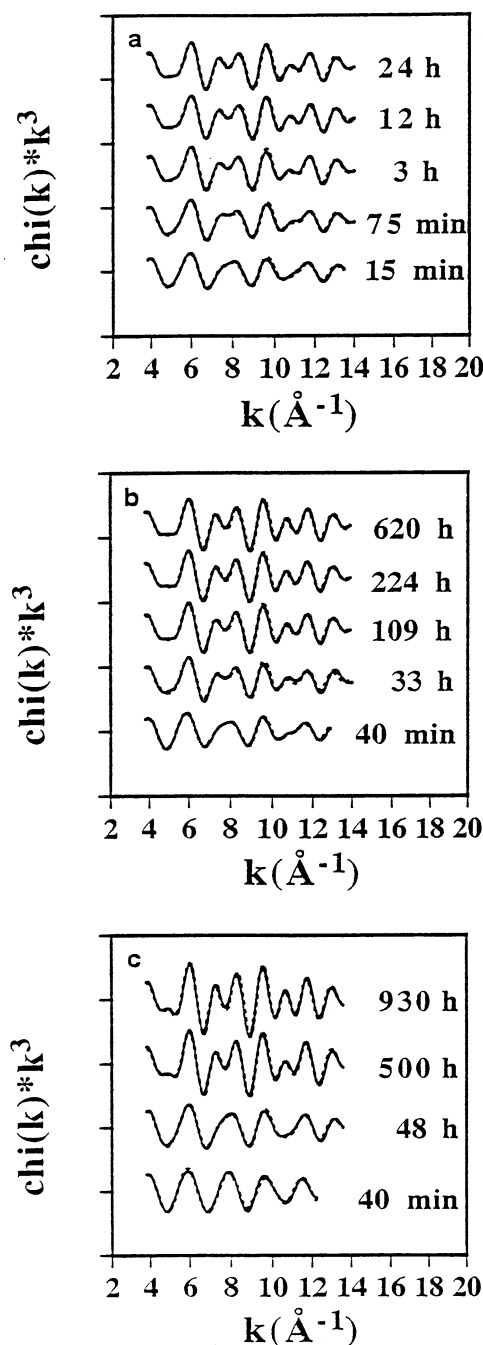
Fig. 3. k^3-weighted XAFS functions (solid line) for the Fourier back-transformed spectra of Ni sorbed on (a) pyrophyllite, (b), gibbsite, and (c) montmorillonite in comparison with the theoretical spectra derived from data analysis (dashed line).

k-space and r-space range of interest removes the asymmetric feature.

3.3. Identification of Sorption Phase and Comparison with Reference Compounds

Table 2 shows the structural parameters of β-Ni(OH)$_2$, takovite (Ni$_6$Al$_2$(OH)$_{16}$CO$_3 \cdot$ H$_2$O), and Ni/Al phases formed by

a coprecipitation process of Ni and Al. An important characteristic of mixed Ni/Al phases is the reduction of the Ni-Ni bond distances compared with those in Ni(OH)$_2$. A similar reduction of the Ni-Ni bond distances can be observed in our Ni sorption samples (Table 3–5). Furthermore, the structural environment in our sorption samples is similar to mixed Ni/Al phases formed upon Ni sorption on γ-Al$_2$O$_3$ (R$_{(Ni-Ni)}$ = 3.04–3.07 Å; d'Espinose de la Caillerie et al., 1995). Thus we propose that mixed Ni/Al hydroxide formation is the predominate sorption mode in our systems.

4. DISCUSSION

4.1. Nickel Sorption During the First Fast Reaction Step (Minutes–Hours)

Nickel sorption kinetics on pyrophyllite, gibbsite, and montmorillonite was initially fast occurring on time scale of minutes The fast sorption step was then followed by a much slower second sorption step which seemed to continue until Ni removal from solution was complete (Fig. 1). The observed sorption kinetics are common for heavy metal sorption on clay and oxide surfaces (Kinniburgh and Jackson, 1981; Brümmer et al., 1988). Traditionally, adsorption (strictly a two-dimensional process) is considered to be the predominant sorption mode responsible for metal uptake on mineral surfaces within the first few minutes to hours, while surface precipitation and/or nucleation processes are considered to be much slower processes, occurring on time scales of hours to days (Sparks, 1989, 1995, 1998a,b; Scheidegger and Sparks, 1996a).

We used XAFS to address the question of whether it is possible to distinguish between a fast metal adsorption step and slower metal nucleation processes (in our case a mixed Ni/Al hydroxide phase). It must be realized that in addition to being incorporated in mixed Ni/Al hydroxide compounds, Ni can bind specifically to Al-OH and/or Si-OH sorption sites of pyrophyllite, gibbsite, and montmorillonite and nonspecifically to permanent-charge sites of montmorillonite.

Our study reveals that Ni sorption on pyrophyllite and gibbsite at pH = 7.5 resulted in the presence of a mixed Ni/Al phase within min (15 min Ni/pyrophyllite and 40 min Ni/gibbsite; Tables 3–4). These findings suggest that adsorption and nucleation processes (mixed Ni/Al phase formation) can occur over similar time scales. The study of Ni sorption on montmorillonite reveals that our finding of a fast growing mixed Ni/Al phase in the Ni/pyrophyllite and Ni/gibbsite systems cannot be extrapolated to other sorption systems. The presence of a mixed Ni/Al phase was not observed for the Ni/montmorillonite system after a reaction time of 40 min. Instead, a reaction time of 48 h was required before a second Ni shell was observed.

Table 5 reveals approximately 6 O atoms at a distance of 2.05 Å for the montmorillonite sample treated with Ni for 40 min. Nickel can adsorb specifically to Al-OH and Si-OH sorption sites of montmorillonite. In the case of Ni sorption on pyrophyllite, bidendate binding of Ni to nonbridging Al-OH surface sites has been suggested as a possible sorption mode at low initial Ni concentrations in order to explain a Ni-Al distance of 2.96 Å (Scheidegger et al., 1996a). Montmorillonite is structurally related to pyrophyllite and thus bidendate binding of Ni to nonbridging Al-OH surface sites also represents a

possible sorption mode for the fast sorption step on montmorillonite. Data analysis of the montmorillonite sample treated with Ni for 40 min does not suggest the presence of second shell backscatterer atoms (Fig. 2f, Table 5). Nevertheless, it should be realized that the XAFS signal is not very sensitive towards a small number (e.g., <0.5) of weak second shell backscatterer atoms like Al and Si.

Nickel can also adsorb onto the internal permanent-charge sites of montmorillonite. An XAFS study on Co sorption on montmorillonite revealed, that both, outer-sphere, mononuclear surface complexes with internal permanent-charge sites and specifically bound, mononuclear Co complexes with surface hydroxyl sorption sites can occur, depending on the pH and the ionic strength (Papelis and Hayes, 1996). At neutral pH (pH = 7) and low ionic strength (I = 0.001 M) a single Co-O distance of 2.09 Å was observed. Under these reaction conditions Co affinity for surface-hydroxyl sites is moderate and the internal permanent-charge sites are accessible. Cobalt sorbed predominantly at permanent-charge sites because the edge surface area of the crystallites is only approximately 2% of the internal surface area (Papelis and Hayes, 1996).

At higher ionic strength, a Co-Co backscattering contribution was observed under reaction conditions (pH = 7; I = 0.1, and 1 M; reaction time >24h) similar to those employed in the present study (pH = 7.5; I = 0.1 M; reaction time for appearance of a mixed Ni/Al phase >48 h). Papelis and Hayes (1996) concluded that with increasing ionic strength Co is increasingly excluded from the interlayer permanent-charge sites and forms polynuclear surface phases. Similar to our study, Co-Co distances (3.12–3.13 Å) agree well with those for synthesized mixed Co-Al hydroxide phases (3.12 Å, Allmann, 1970; 3.08–3.09 Å, d'Espinose de la Caillerie et al., 1995; 3.09 Å, Towle et al., 1997) but were distinctively shorter than in crystalline Co(OH)$_2$(s) (3.17 Å; O'Day et al., 1994a,b; d'Espinose de la Caillerie et al., 1995). Thus, we suspect that the formation of a mixed cation hydroxide-like phase is also a plausible explanation for the reduction of Co-Co distances.

4.2. Nickel Sorption During the Second Slower Reaction Step (Hours–Months)

The Ni sorption kinetics strongly depend on the mineral surface present. For the Ni/pyrophyllite system the Ni uptake reaction is nearly completed within 24 h (97% sorbed, Table 3). The XAFS data of a sample which was treated with Ni for 3 months under similar reaction conditions suggest, however, that there is a tendency towards an increased $N_{(Ni-Ni)}$ beyond a reaction time of 24h (Table 3). We suspect that this finding might be caused by a further increase in the size of the mixed Ni/Al hydroxide phase, perhaps due to a slow restructuring process. For the Ni/gibbsite and Ni/montmorillonite systems the uptake reactions are much slower and a reaction time of ≈1–2 months is required until most Ni is removed from solution. Constant Ni sorption rates are observed for the second sorption step in the Ni/gibbsite and Ni/montmorillonite system (Fig. 1b-c). The solid lines in the figures represent a linear fit of the data set over the time range of 40 min to 620 h for gibbsite and 26 to 930 h for montmorillonite. For both systems a linear fit describes the data well (R^2 = 0.998 for the Ni/gibbsite and R^2 = 0.995 for the Ni/montmorillonite system). The Ni sorp-

tion rates for the second sorption step are 4.5×10^{-12} mol m^{-2} s^{-1} for the Ni/gibbsite system and 4.9×10^{-14} mol m^{-2} s^{-1} for the Ni/montmorillonite system. XAFS data analysis reveals that as the reaction time increased, the number of Ni second-neighbor (N) atoms increased in all sorption systems (Table 3–5). This finding suggests the continuous growth of a mixed Ni/Al hydroxide phase with progressing reaction time.

4.3. What is the Rate-Limiting Step?

The rates of mixed Ni/Al hydroxide formation are affected by pH, the initial Ni/Al ratios in solution, and the types of anions that are present (Allmann, 1970; Taylor, 1984, Cavani et al., 1991). Taylor (1984) found that the rate of mixed Ni/Al hydroxide formation was lower, by a factor of ≈4, as the initial Ni/Al ratio in solution increased from 4 to 8. Even though the rate was lower, mixed Ni/Al hydroxides formed in 1–10 h at 298K (Taylor, 1984).

The present study suggests that the formation of a mixed Ni/Al phase in our sorption samples proceeded much longer (up to 2 months). This finding indicates that the Ni nucleation is not the rate-limiting step. We propose that the dissolution of the sorbent is the rate-controlling factor for the formation of mixed Ni/Al hydroxides in our samples. Aluminum needs to be released into solution before it can be incorporated into a mixed Ni/Al sorption phase.

A previous study (Scheidegger et al., 1997) in our laboratory demonstrated that mineral dissolution (Si release) in a Ni/pyrophyllite sorption system ([Ni]$_o$ = 3mM, pH = 7.5, I = 0.1M) was enhanced compared to the dissolution of the clay alone (Ni-untreated pyrophyllite). Silicon release coincided with Ni removal from solution. For example, the Si concentration in solution was increased by a factor of approximately 5 within the first 12 h of the reaction (5.8×10^{-12} mol m^{-2} s^{-1} vs. 1.3×10^{-12} mol m^{-2} s^{-1}, Scheidegger et al., 1997). This finding indicates that metal sorption on pyrophyllite promotes the dissolution of the clay. It can be argued that clays and aluminum oxides are often coated with an amorphous aluminum hydroxide or aluminum silicate layer (Fritzpatrick, 1980) which could have a significant effect on the (initial) dissolution rates. Nevertheless, in the above mentioned pyrophyllite study (Scheidegger et al., 1997), the same clay material was used and the experiments were performed at identical reaction conditions (pH, ionic strength, hydration time, experimental setup). Thus the observed enhancement of the dissolution rate must be due to Ni addition and cannot be an experimental artifact (e.g., dissolution of an amorphous Al layer formed during the preparation of the minerals).

The [Al] in solution was too low (<50 ppb) to produce reliable ICP measurements in our study. Nevertheless, we suspect that mineral dissolution is also metal ion promoted in the Ni/gibbsite and the Ni/montmorillonite systems. Ideally one would like to estimate the average Al dissolution rate in the sorption samples based on the Ni/Al ratios as determined by XAFS. An accurate determination of the Ni/Al ratio by XAFS is, however, problematic due to the uncertainty in $N_{(Ni-Al)}$ (see section 2). As an alternative one can estimate the average Al dissolution rate based on Ni/Al ratios in mixed Ni/Al hydroxide compounds reported in the literature. Mixed Ni/Al hydroxide compounds have been synthesized from Ni and Al salts over a

wide range of reaction conditions (pH = 5–10.5, initial Ni/Al ratios in solution (0.3–8) and anions present (e.g., Br^-, NO_3^-, OH^-, ClO_4^-, and CO_3^{2-}; Allmann, 1970; Brindley and Kikkawa, 1979; Hashi et al., 1983; Taylor, 1984, Cavani et al., 1991, d'Espinose de la Caillerie et al., 1995). Even though mixed metal hydroxide or carbonate-hydroxide compounds are notorious for substitution, poor crystallinity and variable stoichiometry, the Ni/Al ratios in the resulting mixed Ni/Al solid phases varied predominately between 2 and 4 and were never smaller then 1.3 and never exceeded 5.6 (Brindley and Kikkawa, 1979; Taylor, 1984). For comparison, the Ni/Al ratio commonly found in natural takovites varies between 2.5 and 2.8 (Bish and Brindley, 1977).

Using the Ni sorption rates given in Section 4.2 and assuming the Ni/Al ratios in our sorption samples are within the range of Ni/Al ratios found in the literature (1.3–5.6) one can estimate an average Al dissolution rate between $3.4–0.9 \times 10^{-12}$ mol m^{-2} s^{-1} for the Ni/gibbsite system and approximately $3.8–1 \times 10^{-14}$ mol m^{-2} s^{-1} for the Ni/montmorillonite system. The estimated dissolution rates for the Ni/gibbsite and Ni/montmorillonite systems seem to be enhanced compared to the Al dissolution rates of the minerals alone. The dissolution rate of montmorillonite determined under similar conditions is 1×10^{-15} mol m^{-2} s^{-1} (pH = 6; Heydemann, 1966). We could only find dissolution rates for gibbsite in the literature under acidic pH conditions (5×10^{-13} mol m^{-2} s^{-1} (pH = 3.8, Mogollon et al., 1996); 1.5×10^{-12} mol m^{-2} s^{-1}; pH = 3.8, Bloom and Erich, 1987). The measurement of the dissolution rates of aluminum oxides at neutral or near neutral pH requires the addition of organic agents which readily complex aluminum and prevent the precipitation of an aluminum hydroxide phase (Carroll-Webb and Walther, 1988). Dissolution rates of aluminum oxides at neutral pH are, therefore, uncommon in the literature. Carroll-Webb and Walther (1988) found that the dissolution rate of corundum ($-Al_2O_3$) showed a minimum near pH = 8 (2×10^{-15} mol m^{-2} s^{-1}, I = 0.05 M) and was significantly smaller at neutral pH than at lower pH (e.g., 4×10^{-14} mol m^{-2} s^{-1}, pH = 4, I = 0.05 M).

The finding of an (apparently present) enhancement of Al dissolution due to Ni addition in our study agrees with the results from a study on Ni(II) sorption on a fine powdered, high surface area γ-Al_2O_3 (d'Espinose de la Caillerie et al., 1995). This XAFS study revealed the presence of a mixed Ni/Al hydroxide phase when γ-Al_2O_3 was treated with Ni at neutral or slightly alkaline pH (pH = 7–9). By comparing the dissolution rate of γ-Al_2O_3 with the Al dissolution rate calculated based on Al content in the coprecipitates, the authors found that the addition of Ni(II) enhanced the rate of alumina dissolution (through the formation of the mixed Ni/Al phase) by a factor of more than three orders of magnitude (d'Espinose de la Caillerie et al., 1995).

Ligand promoted enhancement of the dissolution rates of minerals is well-known in the literature (Grauer and Stumm, 1982; Furrer and Stumm, 1986; Wieland et al., 1988; Stumm and Wollast, 1990; Stumm, 1992; Biber et al., 1994; Brady and House, 1996; Drever and Stillings, 1997; Stumm, 1997). For example, inorganic and organic ligands such as phosphate, arsenate, chloride, fluoride, citrate, salicylate, and oxalate are known to accelerate the dissolution of oxides (Grauer and Stumm, 1982; Furrer and Stumm, 1986). Best known in the literature is H^+ and OH^- promoted dissolution (Stumm, 1992; Brady and House, 1996). A high degree of surface protonation of the surface hydroxyl groups accelerates the dissolution because it leads to highly polarized interatomic bonds in the immediate proximity of the surface central ions and thus facilitates the detachment of a cationic surface group into solution (Stumm and Wollast, 1990; Biber et al., 1994). An important question is then, are adsorbed metals [like Ni(II)] able to weaken underlying Al-O bonds at the mineral surface, for example, by polarizing the distribution of charges at some depth in the mineral surface (d'Espinose de la Caillerie et al., 1995). Often it is found that cations such as Cr(III) and Al(III) act as blocking agents of surface functional groups and tend to retard mineral dissolution (Stumm and Wollast, 1990; Stumm, 1997). However, metal promoted dissolution of silicate and oxide minerals noticed by d'Espinose de la Caillerie et al. (1995) and by our laboratory (this study and Scheidegger et al., 1997) is a rather surprising finding which clearly needs further detailed investigations.

4.4. Effect of Surface Loading

Assuming closest-packing of NiO_6 polyhedra on the surface, monolayer coverage corresponds to 11.48 sites nm^{-2} or 19.04 μmol m^{-2}. In the Ni/pyrophyllite system we observed the presence of a mixed Ni/Al phase at a surface loading as low as 0.7 μmol m^{-2} which corresponds to <5% of monolayer coverage (Table 3). The data suggest similar findings for the Ni/gibbsite and the Ni/montmorillonite systems. Nickel sorption on the gibbsite surface resulted in the appearance of a mixed Ni/Al phase at a surface loading of 1 μmol m^{-2} while in the Ni/montmorillonite system the presence of a mixed Ni/Al phase could be discerned at a surface loading of 0.19 μmol m^{-2} (total surface area) and 8.9 μmol m^{-2} (edge surface area only). Again, if the closest-packing of NiO_6 polyhedra is assumed to constitute a monolayer of Ni atoms, the presence of a mixed Ni/Al phase was determined at $\approx$5% monolayer coverage for gibbsite and at $\approx$1% monolayer coverage (total surface area) or <50% monolayer coverage (edge surface area only) for montmorillonite. These findings suggest that surface crowding is not responsible for the formation of a mixed Ni/Al phase in our sorption systems. The appearance of a second shell at fairly low surface coverage is consistent with the results from previous XAFS studies on Co sorption on aluminum oxides and clays. The onset of multinuclear complex formation was observed at coverages as low as 5–10% (O'Day et al., 1994a,b, 1996; Papelis and Hayes, 1996).

In an earlier investigation, employing high-resolution transmission electron microscopy (HRTEM), we showed that the surface structure of pyrophyllite was changed after reaction with Ni at pH = 7.5 (Scheidegger et al., 1996b). Along the edges of the pyrophyllite surface, rough, scalloped cauliflower-like deposits were observed. Thus, we believe the mixed cation hydroxide phases are principally associated with mineral surfaces and do not occur as separate, homogeneous precipitated phases. Furthermore, a recent in situ atomic force microscopy (AFM) study of Ni sorption onto pyrophyllite in our laboratory revealed the growth of surface precipitates growing in size with increasing reaction time (Scheckel et al., 1998). These findings

further suggest the formation of mixed Ni/Al phases over time that were observed in the present study.

In a study on Co sorption on Al_2O_3, however, the presence of a mixed Co/Al hydroxide phase was observed which was associated with the Al_2O_3 substrate, but did not form a coating. Furthermore, there was no evidence for an epitaxial relationship between the precipitate and the mineral substrate (Towle et al., 1997). In another study on Ni sorption onto aluminum oxides d'Espinose de la Caillerie et al. (1995) observed the presence of a mixed Ni/Al coprecipitate not only associated with the surface but also at a distance from the mineral substrate. In their study a 10^{-2} M Ni(II) solution at pH = 9 was added dropwise outside a dialysis bag containing high surface area γ-Al_2O_3 spheres. A green-bluish cloud appeared progressively (over the course of 2 weeks) inside and outside the dialysis bag. Analysis of the coprecipitate showed that the phase consisted of 32 wt% Ni and 10 wt% Al. Furthermore, the thermogravimetric profile of the coprecipitate was found to be very similar to that of hydrotalcite (d'Espinose de la Caillerie et al., 1995). The authors proposed that hydrotalcite nuclei were formed in the vicinity of the alumina surface, and then were free to move away from the surface, under the effect of agitation, in particular through the membrane.

5. CONCLUSIONS

The spectroscopic and kinetic data presented in this paper convincingly show that mixed-cation hydroxide phases occur on an array of clay and oxide mineral surfaces, often forming on time scales of minutes. It appears that the formation of these phases is effected by the addition of a metal cation, such as Ni, to an environment that contains a source of a hydrolyzed species such as Al(III). Our data suggest that three phenomena occur at the mineral/liquid interface: (1) nonspecific and/or specific adsorption; (2) dissolution of Al which is the rate-limiting step whereas the dissolution rate is most probably dependent on the surface morphology and impurities present; and (3) nucleation of a mixed Ni/Al phase.

Some have speculated that the degree to which mixed-cation hydroxide compounds actually do form in aquatic and terrestrial environments is limited more by low rates of soil mineral dissolution, a necessary preliminary step, than by lack of thermodynamic favorability (McBride, 1994). Because the dissolution rates of clays and oxide minerals are fairly slow, the possibility of mixed-cation hydroxide formation as a plausible sorption mode in 24h-based sorption experiments (and also most long-term studies) containing divalent metal ions such as Mg(II), Ni(II), Co(II), Zn(II), and Mn(II) and Al(III)−, Fe(III)−, and Cr(III)-(hydr)oxide or silicate minerals has been ignored in the literature. This study and others recently published (d'Espinose de la Caillerie et al., 1995; Scheidegger et al., 1997), however, suggest that metal sorption onto mineral surfaces can significantly destabilize surface metal ions (Al and Si) relative to the bulk solution, and therefore lead to an enhanced dissolution of the clay and oxide minerals. Thus, predictions on the rate and the extent of mixed-cation hydroxide formation in aquatic and terrestrial environments based on the dissolution rate of the mineral surface alone are not valid and underestimate the true values.

The frequent observations that metal sorption on mineral

surfaces increases slowly with time and that increased residence time decreases the rate and quantity of metal release may be attributable in part to the formation of mixed-cation hydroxide-like phases (Kuo and Mikkelsen, 1980; Benjamin and Leekie, 1981; Padmanabham, 1983; Lehman and Harter, 1984; Davis et al., 1987; Schultz et al., 1987; Brümmer et al., 1988; Barrow et al., 1989; Ainsworth et al., 1994). Scheidegger and Sparks (1996b) showed that metal release from mixed Ni-Al hydroxide phases formed on pyrophyllite was much slower than from crystalline $Ni(OH)_2(s)$ reference compounds. This observation clearly indicates the potential significance of mixed-cation hydroxide phase formation on the fate of metal contaminants in the environment.

This study has emphasized the importance of combining time-dependent or kinetics studies with spectroscopic investigations to better understand sorption processes at the solid/liquid interface. We have demonstrated that this combination can result in a detailed mechanistic understanding (e.g., distinguishing the rate of metal adsorption vs. nucleation processes in sorption systems) which could never have been provided by a macroscopic approach alone.

REFERENCES

Ainsworth C. C., Pilou J. L., Gassman P. L., and Van Der Sluys W. G. (1994) Cobalt, cadmium, and lead sorption to hydrous iron oxide: Residence time effect. *Soil Sci. Soc. Amer. J.* **58,** 1615–1623.

Allmann R. (1970) Doppelschichtstrukturen mit brucitaehnlichen Schichtionen $[Me(II)_{1-x}Me(III)_x(OH)_2]^{x+}$. *Chimia* **24,** 99–108.

Amonette J. C. and Zelazny L. W. (ed.) (1994) *Quantitative Methods in Soil Mineralogy.* Soil Sci. Soc. Amer. Misc. Publ.

Baes C. F. and Mesmer R. E. (1976) *The Hydrolysis of Cations.* Wiley.

Bargar J. R., Brown Jr. G. E., and Parks G. A. (1997) Surface complexation of Pb(II) at oxide-water interfaces: I. XAFS and bond-valence determination of mononuclear and polynuclear Pb(II) sorption products on aluminum oxides. *Geochim. Cosmochim. Acta* **61,** 2617–2637.

Barrow N. J., Gerth J., and Bruemmer G. W. (1989) Reaction kinetics of the adsorption and desorption of nickel, zinc, and cadmium by goethite: II. Modelling the extent and rate of reaction. *Soil Sci.* **40,** 437–450.

Benjamin M. M. and Leckie J. O. (1981) Multi-site adsorption of cadmium, cobalt, zinc, and lead on amorphous iron oxyhydroxide. *J. Colloid Interf. Sci* **79,** 209–221.

Biber M. V., Dos Santos Afonso M., and Stumm W. (1994) The coordination chemistry of weathering: IV. Inhibition of the dissolution of oxide minerals. *Geochim. Cosmochim. Acta* **58,** 1999–2010.

Bish D. L. and Brindley G. W. (1977) A reinvestigation of takovite, a nickel aluminum hydroxy-carbonate of the pyroaurite group. *Amer. Mineral.* **62,** 458–464.

Bloom P. R. and Erich M. S. (1987). Effect of solution composition on the rate and mechanism of gibbsite dissolution in acid solutions. *Soil Sci. Soc. Amer. J.* **51,** 1131–1136.

Bouldin C., Elam T., and Furenlid L. (1995) MacXAFS - An EXAFS analysis package for Macintosh. *Physica B* **208/209,** 190–192.

Boyanov B. (1997) XFTools Collection, unpublished. Source codes and executables are available at http:/ncstarg.physics.ncsu.edu/xftools.

Brady P. V. and House W. A. (1996) Surface-controlled dissolution

and growth of minerals. In *Physics and Chemistry of Mineral Surfaces* (ed P. V. Brady), pp. 225–305. CRC Press.

Brindley G. W. and Kikkawa S. (1979) A crystal-chemical study of Mg,Al and Ni,Al hydroxy-perchlorates and hydroxy-carbonates. *Amer. Mineral.* **64,** 836–843.

Brümmer G. W., Gerth J., and Tiller K. G. (1988) Reaction kinetics of the adsorption and desorption of nickel, zinc and cadmium by goethite: I. Adsorption and diffusion of metals. *J. Soil Sci.* **39,** 37–52.

Bunker G. (1988) *Basic Techniques for EXAFS.* Beamline X-9 documentation.

Carroll-Webb S. A. and Walther J. V. (1988) A surface complex reaction model for pH–dependence of corundum and kaolinite dissolution rates. *Geochim. Cosmochim. Acta* **52,** 2609–2623.

Carter D. L., Heilman M. D., and Gonzalez C. L. (1965) Ethylene glycol monoethyl ether for determining surface area of silicate minerals. *Soil Sci.* **100,** 356–360.

Cavani F., Trifiro F., and Vaccari A. (1991) Hydrotalcite-type anionic clays: Preparation, properties and applications. *Catalysis Today* **11,** 173–301.

Charlet L. and Manceau A. (1992) X-ray absorption spectroscopic study of the sorption of Cr(III) at the oxide-water interface. II: Adsorption, coprecipitation and surface precipitation on ferric hydrous oxides. *J. Colloid Interf. Sci.* **148,** 443–458.

Davis J. A., Fuller C. C., and Cook A. D. (1987) A model for trace metal sorption processes at the calcite surface: Adsorption of Cd^{2+} and subsequent solid solution formation. *Geochim. Cosmochim. Acta* **51,** 1477–1490.

Drever J. I. and Stillings L. L. (1997) The role of organic acids in mineral weathering. *Coll. Surfaces* **120,** 167–181.

d'Espinose de la Caillerie J. B., Kermarec M., and Clause O. (1995) Impregnation of γ-alumina with Ni(II) and Co(II) ions at neutral pH: Hydrotalcite-type coprecipitate formation and characterization. *J. Amer. Chem. Soc.* **117,** 11471–11481.

Evans B. W. and Guggenheim S. (1988) Talc, pyrophyllite, and related minerals. *Rev. Mineral.* **19,** 225–293.

Fendorf S. E., Lamble G. M., Stapleton M. G., Kelley M. J., and Sparks D. L. (1994) Mechanisms of chromium(III) sorption on silica. 1. Cr(III) surface structure derived by extended X-ray absorption fine structure spectroscopy. *Environ. Sci. Technol.* **28,** 284–289.

Fritzpatrick E. A. (1980) *Soils. Their Formation, Classification and Distribution.* Longman.

Fuller C. C., Davis J. A., and Waychunas G. A. (1993) Surface chemistry of ferrihydrite: Part 2. Kinetics of arsenate adsorption and coprecipitation. *Geochim. Cosmochim. Acta* **57,** 2271–2282.

Furrer G. and Stumm W. (1986) The coordination chemistry of weathering: I. Dissolution kinetics of δ-Al_2O_3 and BeO. *Geochim. Cosmochim. Acta* **50,** 1847–1860.

Grauer R. and Stumm W. (1982) Die Koordinationschemie oxidischer Grenzflaechen und ihre Auswirkung auf die Aufloesungskinetik oxidischer Festphasen in waessrigen Loesungen. *Colloid Polym. Sci.* **260,** 959–970.

Hashi K., Kikkawa S., and Koizumi M. (1983) Preparation and properties of pyroaurite-like hydroxy minerals. *Clays Clay Miner.* **31,** 152–154.

Heydemann A. (1966) Ueber die chemische Verwitterung von Tonmineralien (Experimentelle Untersuchungen). *Geochim. Cosmochim. Acta* **30,** 995–1035.

Hiemstra T., van Riemsdijk W. H., and Bolt G. H. (1989) Multisite proton adsorption modeling at the solid/solution interface of (hydr)oxides: A new approach. 1. Model description and evaluation of intrinsic reaction constants. *J. Colloid Interf. Sci.* **133,** 91–99.

Keren R. and Sparks D. L. (1994) The role of edge surfaces in flocculation of 2:1 clay minerals. *Soil Sci. Soc. Amer. J.* **59,** 430–435.

Kinniburgh D. G. and Jackson M. L. (1981) Cation adsorption by hydrous metal oxides and clay. In *Adsorption of Inorganics at the Solid-Liquid Interface* (ed. M. A. Anderson et al.), pp. 91–160. Ann Arbor Science.

Kuo S. and Mikkelsen D. S. (1980) Kinetics of zinc desorption from soils. *Plant Soil* **56,** 355–364.

Lehmann R. G. and Harter R. D. (1984) Assessment of copper-soil bond strength by desorption kinetics. *Soil Sci. Soc. Amer. J.* **48,** 769–772.

Lewis K. R. and Ratner B. D. (1993) Observation of surface rearrangement of polymers using ESCA. *J. Colloid Interf. Sci.* **159,** 77–85.

Manceau A. and Calas G. (1986) Nickel bearing clay minerals: II. Intracrystalline distribution of nickel: An X-ray absorption study. *Clay Minerals* **21,** 341–360.

Mattigod S. V., Rai D., Felmy A. R., and Rao L. (1997) Solubility and solubility product of crystalline $Ni(OH)_2$. *J. Soln. Chem.* 26, 391–403.

McBride M. B. (1994) *Environmental Chemistry of Soils.* Oxford Univ. Press.

McMaster, W. H., Kerr Del Grande, N., Mallett, J. H., and Hubbell, J. H. (1968) *Compilation of X-ray Cross-Sections.* UCRL-50174. Univ. California.

Mogollon J. L., Ganor J., Soler J. M., and Lasaga A. C. (1996) Column experiments and the full dissolution rate law of gibbsite. *Amer. J. Sci.* **296,** 729–765.

O'Day P. A., Brown Jr. G. E., and Parks G. A. (1994a) X-ray absorption spectroscopy of cobalt (II) multinuclear surface complexes and surface precipitates on kaolinite. *J. Colloid Interf. Sci.* **165,** 269–289.

O'Day P. A., Parks G. A., and Brown Jr G. E. (1994b). Molecular structure and binding sites of cobalt(II) surface complexes on kaolinite from X-ray absorption spectroscopy. *Clay Clay Miner.* **42,** 337–355.

O'Day P. A., Rehr J. J., Zabinsky S. I., and Brown Jr G. E. (1994c) Extended X-ray absorption fine structure analysis of disorder and multiple-scattering in complex crystalline solids. *J. Amer. Chem. Soc.* **116,** 2938–2949.

O'Day P. A., Chisholm-Brause C. J., Towle S. N., Parks G. A., and Brown Jr. G. E. (1996) X-ray absorption spectroscopy of Co(II) sorption complexes on quartz (α-SiO2) and rutile (TiO_2). *Geochim. Cosmochim. Acta.* **60,** 2515–2532.

Oswald H. R. and Asper R. (1977) Bivalent metal hydroxides. In *Preparation and Crystal Growth of Materials with Layered Structures* (ed. R. M. A. Lieth), pp. 72–140. Reidel.

Padmanabham M. (1983) Adsorption-desorption behavior of copper(II) at the goethite-solution interface. *Aust. J. Soil Res.* **21,** 309–320.

Papelis C. and Hayes K. F. (1996) Distinguishing between interlayer and external sorption sites of clay minerals using X-ray absorption spectroscopy. *Coll. Surfaces* **107,** 89–96.

Scheckel K. G., Scheidegger A. M., and Sparks D. L. (1998) Ni(II) precipitation and dissolution kinetics on pyrophyllite: An in situ AFM study. (in prep.).

Scheidegger A. M. and Sparks D. L. (1996a) Critical assessment of sorption/desorption phenomena on natural materials. *Soil Science.* **161,** 813–831.

Scheidegger A. M. and Sparks D. L. (1996b) Kinetics of the formation and the dissolution of nickel surface precipitates on pyrophyllite. *Chem. Geol.* **132,** 157–164.

Scheidegger A. M., Lamble G. M., and Sparks D. L. (1996a) Investigation of Ni adsorption on pyrophyllite: An XAFS study. *Environ. Sci. Technol.* **30,** 548–554.

Scheidegger A. M., Fendorf M., and Sparks D. L. (1996b) Mechanisms of nickel sorption on pyrophyllite: Macroscopic and microscopic approaches. *Soil. Sci. Soc. Amer. J.* **60,** 1763–1777.

Scheidegger A. M., Lamble G. M., and Sparks D. L. (1997) Spectroscopic evidence for the formation of mixed-cation hydroxide phases upon metal sorption on clays and aluminum oxides. *J. Colloid Interf. Sci.* **186,** 118–128.

Schindler P. W. and Stumm W. (1987) The surface chemistry of oxides, hydroxides, and oxide minerals. In *Aquatic Surface Chemistry* (ed. W. Stumm), pp. 83–110. Wiley.

Schultz M. F., Benjamin M. M., and Ferguson J. F. (1987) Adsorption and desorption of metals on ferrihydrite: Reversibility of the reaction and sorption properties of the regenerated solid. *Environ. Sci. Technol.* **21,** 863–869.

Smith R. M. and Martell A. E. (1976) *Critical Stability Constants: Inorganic Complexes.* Plenum Press.

Sparks D. L. (1989) *Kinetics of Soil Chemical Processes.* Academic Press.

Sparks D. L. (1995) *Environmental Soil Chemistry.* Academic Press.

Sparks D. L. (1998a) Kinetics of sorption/release processes on natural surfaces. In *Environmental Particles. Structure and Surface Reactions of Soil Particles* (ed. P. M. Huang et al.), pp. 413–448. Wiley.

Sparks D. L. (1998b) Kinetics of soil chemical phenomena: Future directions. In *Future Prospects for Soil Chemistry* (ed. P. M. Huang et al.); *Soil Sci. Soc. Amer. Spec. Publ.* Soil Sci. Soc. Amer. (in press).

Sposito G. (1986) Distinguishing adsorption from surface precipitation. *In Geochemical Processes at Mineral Surfaces* (ed. J. A. Davis and K. F. Hayes); *ACS Symp. Ser.* **323,** 217–228. ACS.

Stumm W. (1992) *Chemistry of the Solid Water Interface*. Wiley.

Stumm W. (1997) Reactivity at the mineral-water interface: Dissolution and inhibition. *Coll. Surfaces* **120,** 146–166.

Stumm W. and Wollast R. (1990) Coordination chemistry of weathering. *Rev. Geophys.* **28,** 53–69.

Szytula A., Muarasik A., and Balanda M. (1971) Neutron diffraction study of Ni(OH)$_2$. *Phys. Stat. Sol*. **B43,** 125–128.

Taylor R. M. (1984) The rapid formation of crystalline double hydroxy salts and other compounds by controlled hydrolysis. *Clay Miner.* **19,** 591–603.

Teo B. K. (1986) *EXAFS: Basic Principles and Data Analysis*. Springer.

Towle S. N., Bargar J. R., Brown Jr. G. E., and Parks G. A. (1997). Surface precipitation of Co(II) on Al$_2$O$_3$. *J. Colloid Interf. Sci.* **187,** 62–82.

Wagman D. D. et al. (1982) The NBS tables of chemical thermodynamic properties: Selected values for inorganic and C1 and C2 organic substances in SI units. *J. Phys. Chem. Ref. Data* **11** (suppl.), 392.

Waychunas G. A., Rea B. A., Fuller C. C., and Davis J. A. (1993) Surface chemistry of ferrihydrite: Part 1. EXAFS studies of the geometry of coprecipitated and adsorbed arsenate. *Geochim. Cosmochim. Acta* **57,** 2251–2270.

Westall J., Zachary J. L., and Morel F. (1976) MINEQL: A computer program for the calculation of chemical equilibrium composition of aqueous systems. Technical Note 18, Dept. of Civil Eng. MIT.

Wieland E., Wehrli B., and Stumm W. (1988) The coordination chemistry of weathering: III. A generalization on the dissolution rates of minerals. *Geochim. Cosmochim. Acta* **52,** 1969–1981.

Zabinsky S. L., Rehr J. J., Ankudinov A., Albers R. C., and Eller M. J. (1995) Multiple-scattering calculations of x-ray absorption spectra. *Phys. Rev. B Condensed 52,* 2995–3006.